

# *Solar modulation in surface atmospheric electricity*

Article

Accepted Version

Harrison, R. G. and Usoskin, I. G. (2010) Solar modulation in surface atmospheric electricity. *Journal of Atmospheric and Solar-Terrestrial Physics*, 72 (2-3). pp. 176-182. ISSN 1364-6826 doi: <https://doi.org/10.1016/j.jastp.2009.11.006> Available at <https://centaur.reading.ac.uk/5906/>

It is advisable to refer to the publisher's version if you intend to cite from the work. See [Guidance on citing](#).

To link to this article DOI: <http://dx.doi.org/10.1016/j.jastp.2009.11.006>

Publisher: Elsevier

All outputs in CentAUR are protected by Intellectual Property Rights law, including copyright law. Copyright and IPR is retained by the creators or other copyright holders. Terms and conditions for use of this material are defined in the [End User Agreement](#).

[www.reading.ac.uk/centaur](http://www.reading.ac.uk/centaur)

**CentAUR**

Central Archive at the University of Reading

Reading's research outputs online

# Solar modulation in surface atmospheric electricity

R. Giles Harrison

*Department of Meteorology, University of Reading*

*PO Box 243, Earley Gate, Reading RG6 6BB, UK*

*Email: r.g.harrison@reading.ac.uk*

Ilya Usoskin

*Sodankylä Geophysical Observatory*

*P.O. Box 3000, FIN-90014 University of Oulu, Finland*

*accepted for publication in J. Atmospheric and Solar Terrestrial Physics*

*J. Atmos Solar Terr Physics* (2010) **72**, 176-182 <http://dx.doi.org/10.1016/j.jastp.2009.11.006>

## Abstract

The solar wind modulates the flux of galactic cosmic rays impinging on Earth inversely with solar activity. Cosmic ray ionisation is the major source of air's electrical conductivity over the oceans and well above the continents. Differential solar modulation of the cosmic ray energy spectrum modifies the cosmic ray ionisation at different latitudes, varying the total atmospheric columnar conductance. This redistributes current flow in the global atmospheric electrical circuit, including the local vertical current density and the related surface potential gradient. Surface vertical current density and potential gradient measurements made independently at Lerwick Observatory, Shetland, from 1978 to 1985 are compared with modelled changes in cosmic ray ionisation arising from solar activity changes. Both the lower troposphere atmospheric electricity quantities are significantly increased at cosmic ray maximum (solar minimum), with a proportional change greater than that of the cosmic ray change.

*Keywords:* solar-terrestrial coupling; cosmic rays; solar variability; layer cloud charging;

## 1. Introduction

Surface measurements of atmospheric electricity have long been thought to show evidence of solar modulation. Early statistical comparisons of the surface potential gradient and sunspot activity associated with terrestrial magnetism supported this view (Chree, 1906; Bauer, 1925), but physical explanations for correlations were not readily apparent. Surface atmospheric electricity measurements made during the first half of the twentieth century appeared to vary in phase with the 11-year (Schwabe) cycle of solar activity (Israël, 1973), but later work, which identified the importance of cosmic rays, showed an anti-phase response to solar activity. For example, cosmic rays showed a positive correlation with the ionospheric potential during the late 1960s and early 1970s (Mülheisen, 1977; Markson and Muir, 1980; Markson, 1981). Establishing whether the sign and existence of solar effects in atmospheric electricity has varied with time requires study of measurements from a variety of periods and sites.

The global atmospheric electrical circuit (Rycroft et al, 2000) drives current from disturbed weather regions to fair weather regions, through the positively electrified ionosphere. In fair weather regions this causes a small current to flow continuously between the ionosphere and the surface. Variations in the total conductivity of an atmospheric column change the local vertical current density flowing in fair weather regions, and the associated potential gradient

at the surface. As galactic cosmic rays provide the principal source of ionisation causing the conductivity of atmospheric air, solar modulation of cosmic ray ionisation physically links solar activity with the lower atmosphere through atmospheric electricity. The vertical current flow is known to be sustained through regions of water droplets (Bennett and Harrison, 2009), and, specifically, cloudy conditions (Nicoll and Harrison, 2009). If clouds respond to the current flow, modulation of the fair weather vertical current density would provide a potential climate influence, because of the sensitivity of the atmospheric energy balance to cloud properties. Cloud edge charging effects on the microphysics of stratiform clouds from the vertical current density have been suggested (Zhou and Tinsley, 2007; Harrison and Ambaum, 2008).

Atmospheric electricity measurements are rare compared with meteorological measurements, which hampers studies of solar influences. The most abundant measurements made are those of the surface potential gradient (PG), with the vertical conduction current density ( $J_c$ ) measured at only a few sites globally. In general  $J_c$  measurements are preferable as they show much smaller local pollution effects than PG (März and Harrison, 2005), but, as studies into solar effects require long period ( $\sim$  several years to decades) surface atmospheric electricity data, insufficient data duration presents a practical difficulty in separating solar-induced atmospheric electricity changes from other effects. Analysis methods include comparison of transient changes in atmospheric electricity coincident with solar flares (Cobb, 1967) or Forbush cosmic ray decreases (März, 1997), and identification of periodicities characteristic of cosmic rays (e.g. at 1.68 years during the 1980s) in long term PG data (Harrison and März, 2007). Using  $J_c$  data obtained from 1966 to 1977 by Prof. D. Olson over northern Minnesota, Markson and Muir (1980) reported a 30% solar cycle variation in  $J_c$ , in phase with the galactic cosmic ray variation. The difference in phase of response to the solar cycle in Olson's measurements from measurements in the first half of the twentieth century has been attributed to changes in stratospheric aerosol loading following volcanic eruptions (Tinsley, 2005). A further possible explanation is that the earlier measurements were incompletely compensated for surface conductivity variations.

To investigate the phase and magnitude responses to solar changes in lower troposphere atmospheric electricity, a later (1978-1985) series of northern latitude measurements made by the UK Met Office at their Lerwick Observatory (Shetland Islands) is studied here. This island site has little local pollution and frequent rainfall, yielding intermittent periods of fair weather atmospheric electricity conditions. The Lerwick surface  $J_c$  and PG data show properties characteristic of clean air, such as correlated variations of the independently observed  $J_c$  and PG (Harrison and Nicoll, 2008). Good agreement between simultaneous European and atlantic measurements of the global circuit's ionospheric potential and the Lerwick PG has also been observed (Harrison and Bennett, 2007; Rycroft *et al* 2008). Additionally, the PG measured at Lerwick during September 1928 showed similarities with atlantic PG measurements made on cruise VII of the geophysical research ship *Carnegie*, (Harrison, 2004a). The late Lerwick measurements are considered here in terms of solar changes, using a model to calculate the expected solar-induced column ionisation changes above the measurement site (Usoskin and Kovaltsov, 2006).

## **2 Data analysis**

### **(a) Lerwick atmospheric electricity data**

Lerwick Observatory remains an operational geophysical and meteorological site, which, from 1926 to 1985, made routine hourly PG measurements. From 1978 to 1985,  $J_c$  measurements were also made. The PG was measured using a radioactive probe, and  $J_c$  was

measured with a horizontal collecting plate, as described by Harrison and Nicoll (2008). Following their investigation and in common with the Met Office conventions in atmospheric electricity, the 15UT measurements are used here for further analysis. Figure 1 shows time series of the 15UT PG and  $J_c$  from Lerwick in fair weather, throughout the available  $J_c$  measurements. Because of the site's climatology, fair weather periods only occur intermittently and the dataset is sparse with appreciable variability. Robust statistical methods employing threshold tests on median values are therefore used for the analysis. A preliminary aspect is that some seasonality is apparent in the data. The seasonality has been removed by calculating a daily mean value for each day of the year using the available values across the seven years, and fitting a slowly varying (90-day) moving average to the daily mean values found. This smoothed annual cycle was then subtracted from the measured daily values.

From inspection of figure 1 no clear 11-year solar cycle variation is seen, which indicates local variations at the site such as those associated with changes in weather conditions, variations in the application of "fair weather" criteria to the data (or limitations in the criteria), or indeed instrument uncertainties. Calculation of the expected local effects from solar-induced changes in cosmic ray ionisation is used for further investigation of the data.

### (b) Columnar resistance variations at Lerwick

Cosmic ray variations arising from solar activity modify the local volumetric ion production rate  $q$ . In clean air containing bipolar ions with mean mobility  $\mu$ , the total air conductivity  $\sigma$  is given by

$$\sigma = 2\mu e \sqrt{\frac{q}{\alpha}} \quad (1),$$

where  $\alpha$  is the ion-ion recombination coefficient and  $e$  the elementary charge. Analysis of atmospheric electricity changes at Lerwick in the years following nuclear weapon radioactivity deposition showed that the square root dependency of ionisation rate was an appropriate assumption for the site (Pierce, 1972), which illustrates the negligible aerosol concentration present. The conductivity can be integrated with height to determine the total conductance or, more usually, the total resistance. For a unit area column, the columnar resistance  $R_c$  is found from

$$R_c = \int_0^{z_1} \frac{dh}{\sigma(h)} \quad (2),$$

where  $\sigma(h)$  represents the total air conductivity variation with height  $h$  and  $z_1$  is the effective ionospheric height.  $R_c$  varies with latitude and with aerosol concentration (Roble and Tzur, 1986). For the polluted site at Kew, London, experimentally derived  $R_c$  measurements vary from 64 to 310  $\text{P}\Omega \text{ m}^2$  (Harrison, 2005; Rycroft et al, 2008), from which Harrison and Nicoll (2008) estimated  $R_c$  for Lerwick as 70  $\text{P}\Omega \text{ m}^2$ , using a short period of overlapping data.

For equations (1) and (2) to be used to calculate  $R_c$ , the cosmic ray induced ionisation (CRII)  $q$  is required. The CRII can be computed using a numerical model (Usoskin and Kovaltsov 2006), which considers in detail the nuclear-electromagnetic-muon cascade initiated by energetic cosmic ray particles in the atmosphere. Temporal variations of the cosmic ray spectrum are accounted for by using data from the worldwide neutron monitor network

(Usoskin et al., 2005). The model, verified against sporadic direct measurements of CRII (Bazilevskaya et al., 2008), allows the CRII to be computed at a given location and time. To find the CRII for a specific location, the geomagnetic rigidity cut-off is required, which, for Lerwick, is about 0.8 GV. Figure 2 shows the calculated air conductivity using the CRII model (upper panel), and the derived  $R_c$  (lower panel). Much of the variation in air conductivity from cosmic rays occurs in the upper troposphere (upper panel) and lower stratosphere (middle panel), which is where the cosmic ray influence on  $R_c$  dominates.

For figure 2, the air conductivity was found from equation (1) using temperature and pressure profiles to find the local values of  $\alpha$  and  $\mu$  appropriate to the height. For a CRII at standard conditions of  $q_s$  (ion-electron pairs per unit mass per unit time), the local volumetric ion production rate  $q$  was calculated as

$$q = q_s \rho(P, T) \quad (3),$$

where  $\rho$  is the air density found from the gas law for air temperature  $T$  and pressure  $P$ , which each vary with height  $h$ . The local recombination rate and ion mobility were found from

$$\alpha = \alpha_s \left( \frac{293}{T[K]} \right)^{-3.5} \quad (4)$$

and

$$\mu = \mu_s \left( \frac{1013}{P[hPa]} \right) \left( \frac{T[K]}{293} \right) \quad (5)$$

respectively, with  $\alpha_s = 1.6 \times 10^{12} \text{m}^3 \text{s}^{-1}$  (Callahan *et al* 1951) and  $\mu_s = 1.2 \times 10^{-4} \text{m}^2 \text{V}^{-1} \text{s}^{-1}$ . The  $P$  and  $T$  profiles used were: (1)  $P(h)$  was assumed to vary vertically according to an exponential atmosphere profile with scale height 6 km, and (2)  $T(h)$  was assumed to follow a dry adiabatic lapse rate from the surface to 213K, above which the temperature remained constant. With these profiles, the local air conductivity was integrated with height using equation (2) to find  $R_c$ , assuming equation (1), *i.e.* with a negligible effect of local aerosol. The median  $R_c$  value found from the calculations is  $69 \text{ P}\Omega \text{ m}^2$ , close to  $70 \text{ P}\Omega \text{ m}^2$  previously estimated by Harrison and Nicoll (2008). This further supports the clean air assumption made.

### (c) Solar activity variations

During the Lerwick  $J_c$  measurements, solar activity variations modulated the cosmic ray ionisation, which would have varied  $R_c$  above the site. Occasional rapid changes increases in  $R_c$  are apparent, which arise from Forbush decreases in galactic cosmic rays. During  $CR_{\min}$  (solar maximum),  $R_c$  is at its greatest, and during  $CR_{\max}$  (solar minimum),  $R_c$  is at its least. To separate the cosmic ray minimum ( $CR_{\min}$ ) and maximum ( $CR_{\max}$ ) conditions at Lerwick, whilst retaining a considerable amount of the data, the upper 40<sup>th</sup> and lower 40<sup>th</sup> percentiles of  $R_c$  are used (figure 3(a)).

Figure 3 shows the data from figures 1 and divided by days of  $CR_{\min}$  and  $CR_{\max}$ . Firstly, figure 3(b) summarises the effect of splitting the  $R_c$  values; the  $R_c$  values for  $CR_{\max}$  are more skewed than for  $CR_{\min}$ , but using the upper 40<sup>th</sup> and lower 40<sup>th</sup> percentiles the  $CR_{\max}$  and  $CR_{\min}$  values of  $R_c$  become distinct. Figures 3(c) 3(d) show the Lerwick PG and  $J_c$  divided in the same way. From the notches on the boxplots (95% confidence levels), both the PG and  $J_c$ ,

are larger for  $CR_{\max}$  than  $CR_{\min}$ , as expected from the reduced  $R_c$ . As the  $J_c$  and PG distributions are skewed, the differences in the distributions between  $CR_{\max}$  and  $CR_{\min}$  have also been tested using the Mann-Whitney test (Mann and Whitney, 1947). Using this test, the changes in the PG and  $J_c$  distributions are significantly greater than zero with  $p < 0.001$  (confidence level  $> 99.8\%$ ) and  $p < 0.02$  (confidence level  $> 98\%$ ) respectively. In addition to the significant  $CR_{\max}$  to  $CR_{\min}$  changes found in PG and  $J_c$ , it should be noted that the PG and  $J_c$  were measured separately (there are, for example, some days with PG measurements but without  $J_c$  measurements), and that the division into  $CR_{\max}$  and  $CR_{\min}$  categories is independent of the actual atmospheric electricity data.

Table 1 summarises the differences between the  $CR_{\min}$  and  $CR_{\max}$  conditions. Daily measurements from the Climax neutron monitor (NM) for the same time period are also given, divided according to the same  $R_c$  criteria. For the NM, there is an increase of 8.4% from  $CR_{\min}$  to  $CR_{\max}$ , to which  $q$  is approximately proportional. The associated reduction in the calculated  $R_c$  from the CR11 model is smaller (5.1%) than for the NM, due to the clean air assumption causing the square-root dependence in equation (1). (In highly polluted air,  $\sigma$  varies directly with  $q$ , rather than  $q^{1/2}$ .) Both the independently measured atmospheric electrical quantities at Lerwick show a positive change from  $CR_{\min}$  to  $CR_{\max}$  with a change in their medians of 12% in PG and 16.5% in  $J_c$ .

## 2. Related global circuit changes

As for the case of the 1966-1977 Minnesota  $J_c$  data considered by Tinsley (2005), the Lerwick surface atmospheric electricity data appear likely to have increased more substantially with solar activity than expected from modelled columnar resistance changes alone, although their lower bound changes are not incompatible with the modelled columnar resistance change. Further factors are therefore likely to be modulating  $J_c$ , such as local aerosol effects generated by cosmic ray ionisation in the lower troposphere, or changes in current flow in the global circuit. Of those, the first possibility arises as cosmic ray ionisation is thought, in suitable circumstances, to generate ultrafine aerosol particles (*e.g.* Kazil et al 2008). In the lower troposphere, such particle formation would, however, act to remove ions and reduce the air conductivity (Harrison and Carslaw, 2003), increasing the columnar resistance. Cosmogenic aerosol production would therefore act to reduce  $J_c$  at  $CR_{\max}$ , which is opposite to the observed  $J_c$  response. A second possibility is that current flow in the global circuit is redistributed at  $CR_{\max}$ , adding to the local effect of reduced  $R_c$  at Lerwick. Quantitative support exists for this from intensive studies of the ionospheric potential in the 1960s and 1970s (Mülheisen 1971, 1977; Markson and Muir, 1980; Markson, 1981).

### (a) Ionospheric potential modulation

The ionospheric potential,  $V_1$ , is found by integrating the electric field profile vertically, obtained using a balloon or aircraft ascent. As it can be assumed globally to be an equipotential, the sounding position is unimportant. In terms of the conduction current density  $J_c$  measured at the surface, a combined effect of  $V_1$  and  $R_c$  arises through Ohm's Law, *i.e.* from

$$J_c = \frac{V_1}{R_c} \quad (6).$$

Studies of  $V_1$  and NM data (Markson and Muir, 1980; Markson, 1981) showed that  $V_1$  was proportional to neutron count rate, *i.e.* that  $V_1$  increases with cosmic ray ionisation, and therefore, for equation (6), the numerator increases and the denominator decreases with increasing cosmic rays. A reason originally suggested (Markson, 1981) for the relationship with NM counts was the cosmic ray modulation of the above-thunderstorm coupling

resistance. Subsequently the possibility that cosmic rays directly modulate lightning flash rates (with an implied related effect on global circuit currents) has received more attention, although the sign of the relationship remains uncertain and shows strong regional sensitivity (Schlegel et al, 2001).

**(b) Sensitivity to combined global circuit and column changes**

A difficulty in assessing the sensitivity in equation (6) is that the ionospheric potential  $V_1$  has only been sampled intermittently and, furthermore, only some of this data is widely available. The most numerous series of soundings available is that made between 1959 and 1976 by Prof. R. Mühleisen, based in Weissenau, former E. Germany (Mülheisen 1971; 1977). Most of the Mühleisen  $V_1$  radiosonde balloon ascents (from 1959 to 1971) are tabulated in Budyko (1971), together with ascents made during short measurement campaigns from the *Meteor* research ship in the Atlantic. The data tables record the launch time, and the quality of the data determined from a comparison of the  $V_1$  values found from ascent and descent, and the altitude reached. Further soundings in the early 1970s were given in Markson and Muir (1980), from which daily averages were calculated. Only data after the beginning of 1966 is considered, to remove possible stratospheric columnar resistance perturbations of the volcanic eruption during 1963 (Meyerott et al, 1983; Tinsley, 2005) or ionisation effects from atmospheric nuclear tests (Harrison, 2004b). The  $V_1$  dataset is clearly sparse and the available measurements are generally concentrated into periods of intensive observations. Monthly averages have been calculated for those months in which there are four or more measurements available. Monthly average neutron count rates at the Climax NM have also been calculated using the same days' data as the soundings. Figure 4(a) shows time series of  $V_1$  and Climax NM count rates, with calculated monthly averages.

Figure 4(b) shows the monthly averages of  $V_1$  and Climax NM count rate plotted against each other.  $V_1$  increases with neutron count rates and, if the monthly averages are assumed independent of each other, a linear model provides a significant fit to the data. (A correction has been applied to the launch time to obtain the effective sampling time, as explained in Appendix A.) The sensitivity is such that, for a 100% change in Climax neutrons, there is a 154% change in  $V_1$ . This is close to the sensitivity found by Markson (1981), who also used the Mühleisen data, but without excluding the  $V_1$  measurements during the volcanic aerosol period and without including the *Meteor* cruises. Only a few further measurements of  $V_1$  were made up until the early 1980s, which did not show a modulation with cosmic rays (Markson, 1985). It is possible that the solar modulation was not apparent in these later soundings because of insufficient measurements to average out natural variability, unlike the earlier period considered for which many more soundings, although intermittent, are available.

The different sensitivities in the NM and  $V_1$  are likely to result from energy differences between cosmic rays able to affect the global circuit by ionisation compared with those generating secondary particles reaching a surface-located neutron monitor. With such a combination of local and global factors modulating  $J_c$ , the combined sensitivity of  $J_c$  to neutron rate can be estimated from (6) using the quotient rule as

$$\frac{dJ_c}{dC} = \left(\frac{1}{R_c}\right)^2 \left[ R_c \frac{dV_1}{dC} - V_1 \frac{dR_c}{dC} \right] \quad (7)$$

where  $C$  is the Climax NM count rate. The  $V_1$  sensitivity 1966-1972 may not remain appropriate for the 1978-1985 period of the Lerwick data, but, using it with values from Table 1, gives an estimate from equation (7) of a 23% change in  $J_c$  from  $CR_{\min}$  to  $CR_{\max}$ . This

is within the confidence range of the Lerwick changes in  $J_c$  and PG, and broadly consistent with the solar cycle Minnesota  $J_c$  changes of 30%.

#### 4. Discussion and conclusions

Changes in the global circuit's fair weather conduction current are potentially important to cloud properties, as the conduction current may influence the clouds through which it passes. Modulation of the global circuit's current density occurs as a result of solar induced cosmic ray ionisation changes, and this study shows that, from 1978 to 1985, the current density at Lerwick increases with increasing galactic cosmic ray ionisation, with changes between cosmic ray minimum and maximum of 12% in PG and 16.5% in  $J_c$ . This response is consistent with the analysis of Olson's Minnesota measurements from 1966 to 1977, extending the period of a positive response in current density with cosmic rays in northern latitudes to encompass 1966 to 1985. In both cases the observed response in current density was greater than the associated change in neutron monitor measurements of cosmic rays, by two to three times in the case of the Lerwick data.

This increased sensitivity over the neutron monitor change arises because the atmospheric columnar resistance and/or thunderstorm modulation effects on the global circuit respond to lower energy cosmic rays than neutron monitors, which detect secondary particles from energetic collisions. Beyond the different sensitivities of the global circuit and neutron monitors to cosmic rays, the solar modulation of cosmic rays also varies with their energy. There is a greater modulation of the lower energy cosmic rays (an order of magnitude at  $\sim 100$  MeV), compared with higher energy cosmic rays (several per cent at  $\sim 10$  GeV). The Climax neutron monitor has somewhat higher geomagnetic cut-off rigidity ( $\sim 3$  GV compared to 0.8 GV at Lerwick), which also slightly (by a few percent) reduces the solar cycle variation of the Climax data. In summary, the enhanced solar response of the current density over that of neutron monitors results from the different sensitivities of neutron monitors and the global circuit to the local cosmic rays of different energies.

#### Appendix. Effective sampling times

For a balloon sounding of electric field to represent the daily ionospheric potential  $V_1$ , a correction for the  $V_1$  sampling time is required.  $V_1$  is known to vary diurnally with the Carnegie curve, originally determined for oceanic PG measurements. The Carnegie curve variation (as a fraction of the daily mean value  $f_{\text{Carnegie}}$ ) with the UT hour of day  $h$  is given by Israël (1973) as

$$f_{\text{Carnegie}}(h) = 100 + 14.46 \sin \left( 2\pi \left[ \frac{h}{24} + \left( \frac{191.9667}{360} \right) \right] \right) + 4.43 \sin \left( 2\pi \left[ \frac{2h}{24} + \left( \frac{232.85}{360} \right) \right] \right) \quad (\text{A1}).$$

If the balloon sampling time  $h_s$  is known, equation (A1) can be used to correct the  $V_1$  determined to an effective daily mean value. For the Mülheisen balloon ascents, only the UT launch time  $h_0$  is available and consequently  $h_s$  can only be estimated. The practice of Mülheisen was to compare the  $V_1$  values from the ascent and descent soundings for agreement, therefore  $h_s$  was appreciably later than  $h_0$ , depending on the ascent and descent speeds and the balloon burst height. For 26 Weissenau ascents (Gringel, 1978), the most common burst height was 24 km although this varied considerably (standard deviation 8.6 km). Ascent rates vary inversely with burst height and decrease with height above 10 km (HMSO, 1961), but for the 1.1 kg payloads of the Weissenau sondes (Gringel, 1978), typical



mean ascent rates would be 5 to 8 ms<sup>-1</sup> (HMSO, 1961). Assuming similar descent rates, the flight times (allowing for 1 standard deviation on the burst height) would therefore be ~1 to 4 hours. Since the majority of the  $V_1$  sounding occurs in the resistive lower part of the atmosphere, the mean  $V_1$  obtained by averaging the two soundings from ascent and descent would represent  $V_1$  at about 2 to 3.5 hours after launch.

Figure 4(b) shows the relationship between monthly mean neutron count rates and the derived monthly mean  $V_1$  from individual soundings for which the launch time was recorded. Table A1 shows the effect on the linear fit in figure 4(b) of using different lag times from the launch time to correct the  $V_1$  soundings to a daily mean value. For no lag, the fit is significant, but the fit is improved if the lag time is increased to between 3 and 5 hours. For lag times longer than this time, or for negative lag times (*i.e.* an unphysical sampling time of before the launch), the fit is not significant at 95% confidence. The improvement of significance in the linear fit using a sampling time correction suggests that the  $V_1$ -neutron relationship is physically based.

### **Acknowledgements**

The Climax neutron monitor data is supported by the National Science Foundation and the Lerwick atmospheric electricity data were obtained by the Met Office.

## References

- Bauer, L.A., 1925. Correlations between solar activity and atmospheric electricity. *Terr. Mag.* 29, 23-32 and 161-186.
- Bazilevskaya, G.A., Usoskin, I.G., Flueckiger, E.O., Harrison, R.G., Desorgher, L., Buetikofer, R., Krainev, M.B., Makhmutov, V.S., Stozhkov, Y.I., Svirzhevskaya, A.K., Svirzhevsky, N.S., Kovaltsov, G.A., 2008. Cosmic Ray Induced Ion Production in the Atmosphere, *Space Sci. Rev.*, 137, 149-173.
- Bennett, A. J., Harrison, R. G., 2009. Evidence for global circuit current flow through water droplet layers. *J. Atmos. Sol. Terr Phys.* 17, 12, 1219-1221  
<http://dx.doi.org/10.1016/j.jastp.2009.04.011>
- Budyko, M.I., 1971. Results of observations of atmospheric electricity (The World Network, Additional Issue 1965-1969). USSR Chief Administration of the Hydro-Meteorological Service, Leningrad.
- Callahan, R.C., Coroniti, S.C., Parziale A.J., Patten, R., 1951. Electrical conductivity of air in the troposphere. *J. Geophys. Res.* 56, 545-551.
- Chree C., 1906. A discussion of atmospheric electric potential results at Kew from selected days during the seven years 1898 to 1904. *Phil. Trans. Roy. Soc. Lond.* 206, 299-334.
- Cobb, W.E., 1967. Evidence of a solar influence on the atmospheric electric elements at Mauna Loa Observatory. *Monthly Weather Review* 95, 12, 905-911.
- Gringel, W, 1978. Untersuchungen zur elektrischen Leitfähigkeit Berücksichtigung der Sonnenaktivität unter der Aerosolteilchenkonzentration bis 35km Höhe, PhD Thesis, University of Tübingen.
- Harrison, R.G., 2004a. Long term measurements of the global atmospheric electric circuit at Eskdalemuir, Scotland, 1911-1981. *Atmos. Res.* 70 (1), 1-19,  
[10.1016/j.atmosres.2003.09.007](http://dx.doi.org/10.1016/j.atmosres.2003.09.007)
- Harrison, R.G., 2004b. The global atmospheric electrical circuit and climate. *Surveys in Geophysics* 25, (5-6), 441-484, [doi: 10.1007/s10712-004-5439-8](http://dx.doi.org/10.1007/s10712-004-5439-8)
- Harrison, R.G., 2005. Columnar resistance changes in urban air. *J. Atmos. Sol. Terr. Phys* 67 (8-9), 763-773.
- Harrison, R.G., Ambaum, M.H.P., 2008. Enhancement of cloud formation by droplet charging. *Proceedings Royal Society A* 464, 2561-2573. [doi: 10.1098/rspa.2008.0009](http://dx.doi.org/10.1098/rspa.2008.0009)
- Harrison, R.G., Bennett, A.J., 2007. Multi-station synthesis of early twentieth century surface atmospheric electricity measurements for upper tropospheric properties. *Advances in Geosciences* 13, 17-23.
- Harrison, R.G., Carslaw, K.S., 2003. Ion-aerosol-cloud processes in the lower atmosphere. *Reviews of Geophysics* 41 (3), 1012, [doi: 10.1029/2002RG000114](http://dx.doi.org/10.1029/2002RG000114)
- Harrison, R.G., März, F., 2007. Heliospheric timescale identified in surface atmospheric electricity. *Geophys. Res. Lett.* 34, L23816, [doi:10.1029/2007GL031714](http://dx.doi.org/10.1029/2007GL031714)
- Harrison, R.G., Nicoll, K.A., 2008. Air-earth current density measurements at Lerwick; implications for seasonality in the global electric circuit. *Atmospheric Research* 89, 1-2, 181-193, [doi:10.1016/j.atmosres.2008.01.008](http://dx.doi.org/10.1016/j.atmosres.2008.01.008)
- HMSO, 1961. Handbook of Meteorological Instruments, Part II (Instruments for Upper Air Observations), Her Majesty's Stationery Office, London.
- Israël, H., 1973. Atmospheric Electricity vol.2 (Fields, charges, currents) (Problems of Cosmic Physics vol.29), Israel Program for Scientific Translations, Jerusalem.
- Kazil J., Harrison, R.G., Lovejoy, N., 2008. Tropospheric new particle formation and the role of ions. *Space Sci Rev* 137, 241-255 [doi: 10.1007/s11214-008-9388-2](http://dx.doi.org/10.1007/s11214-008-9388-2)
- Mann, H.B., Whitney, D.R., 1947. On a test of whether one of two random variables is stochastically larger than the other. *Annals of Mathematical Statistics*, 18, 50-60.

- März, F., 1997. Short-term changes in atmospheric electricity associated with Forbush decreases, *J. Atm. Solar Terr. Phys.*, 59, (9), 975-982.
- März, F., Harrison, R.G., 2005. Further signatures of long-term changes in atmospheric electrical parameters observed in Europe. *Annales Geophysicae* 23, 6, 1987-1995.
- Markson R., Muir, M., 1980. Solar wind control of the Earth's electric field *Science* 208, 4447, 979-990
- Markson R., 1981. Modulation of the earth's electric field by cosmic radiation *Nature* 291, 304-308.
- Markson, R., 1985. Aircraft measurements of the atmospheric electrical global circuit during the period 1971-1984. *J. Geophys. Res.* 90, D4, 5967-5977.
- Meyerott R.E., Reagan, J.B., Evans, J.E., 1983. On the correlation between ionospheric potential and the intensity of cosmic rays. In *Weather and Climate Responses to Solar Variation*, 449-460, ed. McCormac, B. M., Colorado Associated University Press.
- Mülheisen, R.P., 1971. New determination of the air-earth current over the ocean and measurements of ionospheric potentials. *Pur. App. Geophys.* 84, 112-115.
- Mülheisen, R., 1977. The global circuit and its parameters. In *Dolezalek, H., Reiter, R. (eds), Electrical Processes in Atmospheres*, Steinkopf Verlag, 467-476.
- Nicoll, K.A., Harrison, R.G., 2009. Vertical current flow through extensive layer clouds *J. Atmos. Sol. Terr. Phys.* 71 (12), 1219-1221 [doi:10.1016/j.jastp.2009.09.011](https://doi.org/10.1016/j.jastp.2009.09.011)
- Pierce E.T., 1972. Radioactive fallout and secular effects in atmospheric electricity. *J. Geophys. Res.* 77, 1, 482-487.
- Rycroft, M.J., Israelsson, S., Price, C., 2000. The global atmospheric electric circuit, solar activity and climate change *J. Atmos. Sol Terr. Phys* 62, 1563-1576.
- Rycroft, M.J., Harrison, R.G., Nicoll, K.A., Mareev, E.A., 2008. An Overview of Earth's Global Electric Circuit and Atmospheric Conductivity. *Space Sci Rev* 137, 83-105 [doi: 10.1007/s11214-008-9368-6](https://doi.org/10.1007/s11214-008-9368-6)
- Roble, R., Tzur, I., 1986. in *The Earth's Electrical Environment*, E.P. Krider, R. Roble, Eds (National Academies Press, Washington D.C. 1986), 206-231.
- Schlegel, K., G. Dienforger, S. Thern, M. Schmidt, 2001. Thunderstorms, lightning and solar activity-Middle Europe. *J. Atmos. Sol. Terr. Phys.* 63, 1705-1713.
- Tinsley, B.A. 2005. On the variability of the stratospheric column resistance in the global electric circuit. *Atmos. Res.* 76, 1-4, 78-94.
- Usoskin, I.G., K. Alanko-Huotari, G.A. Kovaltsov, K. Mursula, Heliospheric modulation of cosmic rays: Monthly reconstruction for 1951-2004, 2005. *J. Geophys. Res.*, 110(A12), A12108.
- Usoskin, I. G., and G. A. Kovaltsov, 2006. Cosmic ray induced ionization in the atmosphere: Full modeling and practical applications. *J. Geophys. Res.*, 111, D21206, [doi:10.1029/2006JD007150](https://doi.org/10.1029/2006JD007150).
- Zhou, L., and B.A. Tinsley, 2007. Production of space charge at the boundaries of layer clouds. *J. Geophys. Res.*, 112, D11203, [doi:10.1029/2006JD007998](https://doi.org/10.1029/2006JD007998).

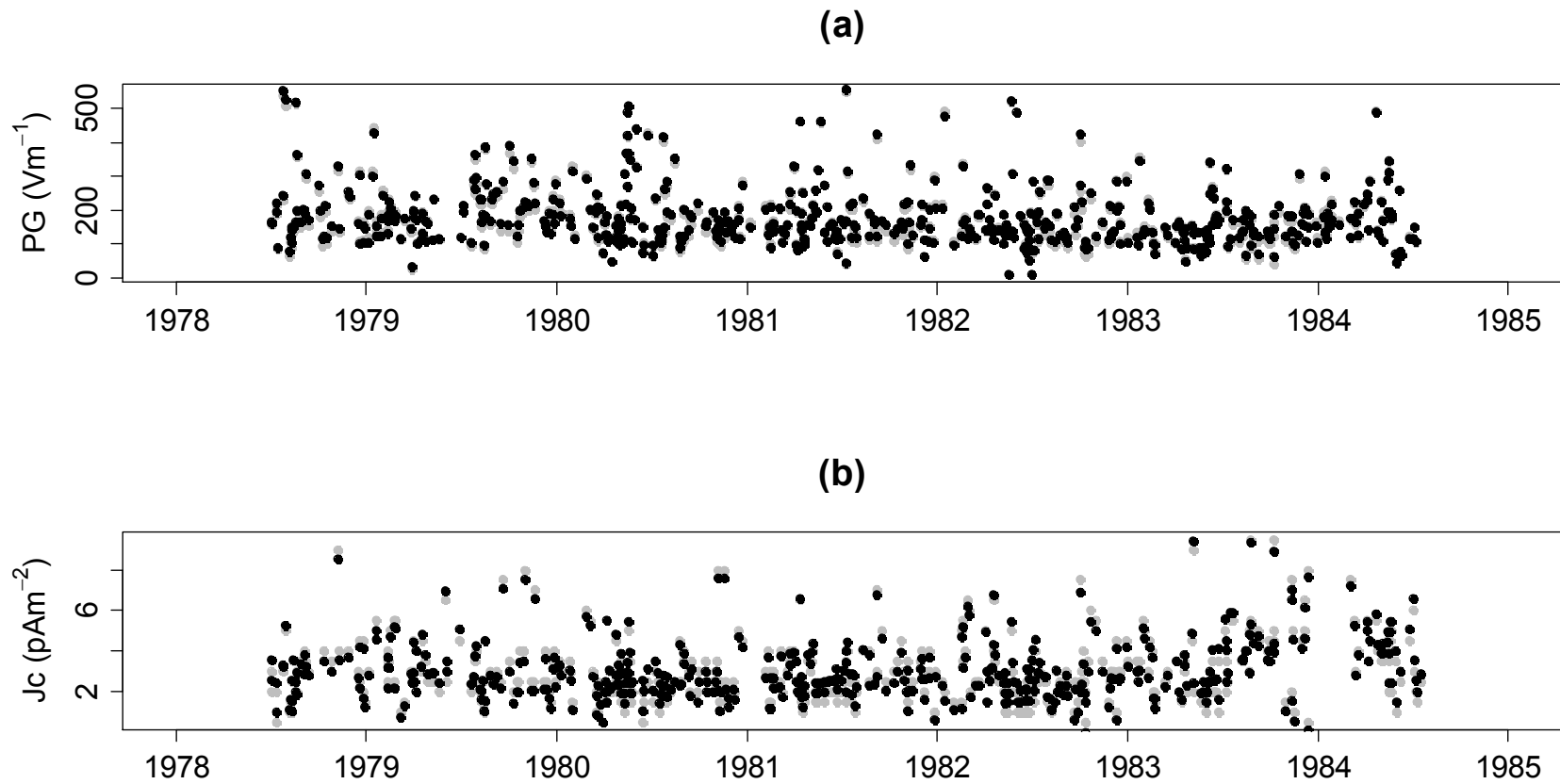


Figure 1. Daily (15UT) fair weather atmospheric electricity measurements at Lerwick. (a) Potential Gradient (PG) and (b) conduction current density ( $J_c$ ). For both plots grey points show the raw data and black points the seasonally corrected values, adjusted by the median of the raw data values.

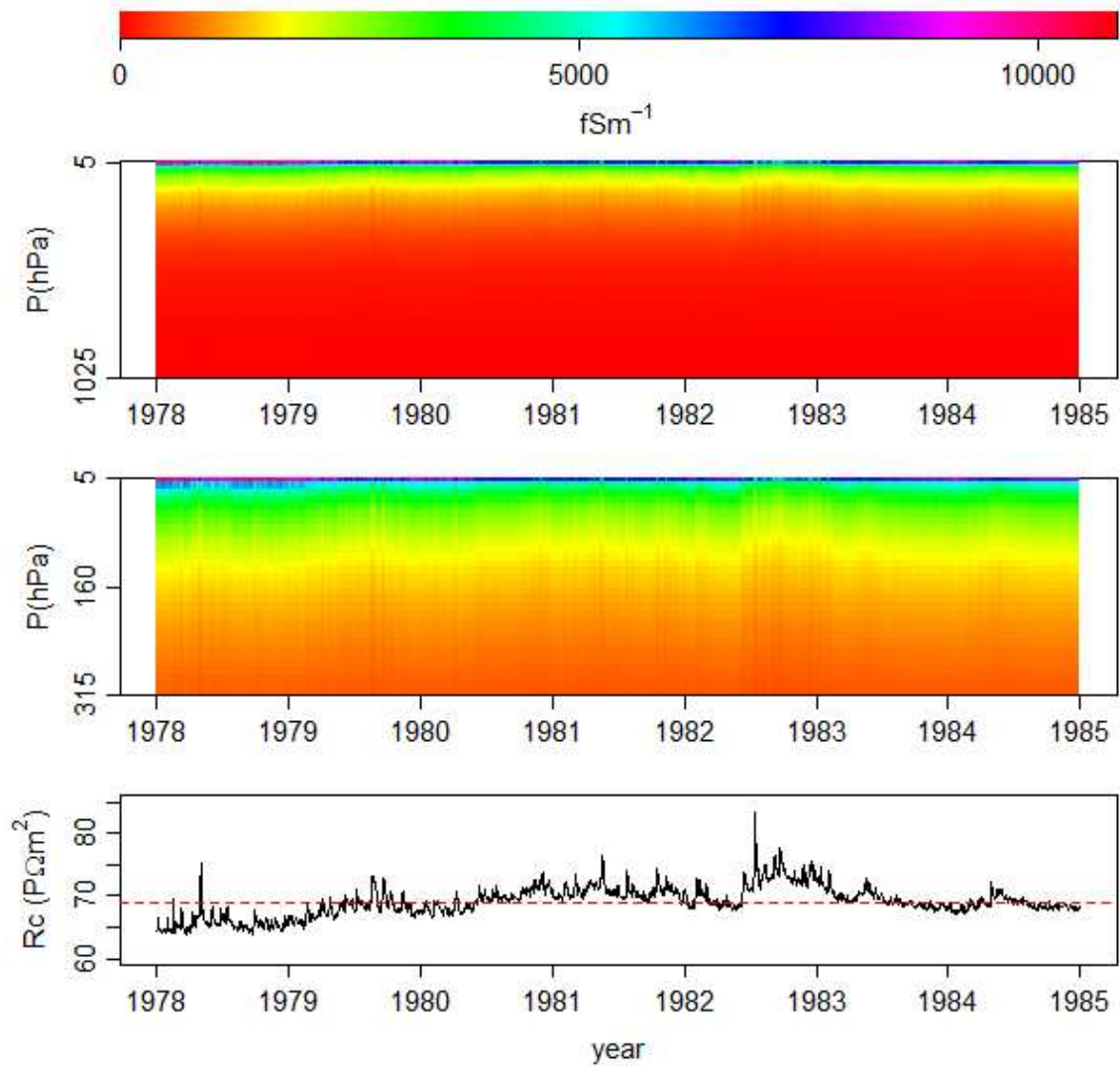


Figure 2. Air conductivity profiles (against atmospheric pressure  $P$ ) for Lerwick 1978-1985 from the CR11 cosmic ray ion-production model. Conductivity time series are shown for the troposphere (upper panel) with the upper troposphere (middle panel), both using the same conductivity scale (top bar). The lower panel shows the surface-stratosphere columnar resistance  $R_c$  derived from integrating the air conductivity profile with height, with the median  $R_c$  marked (dashed line).

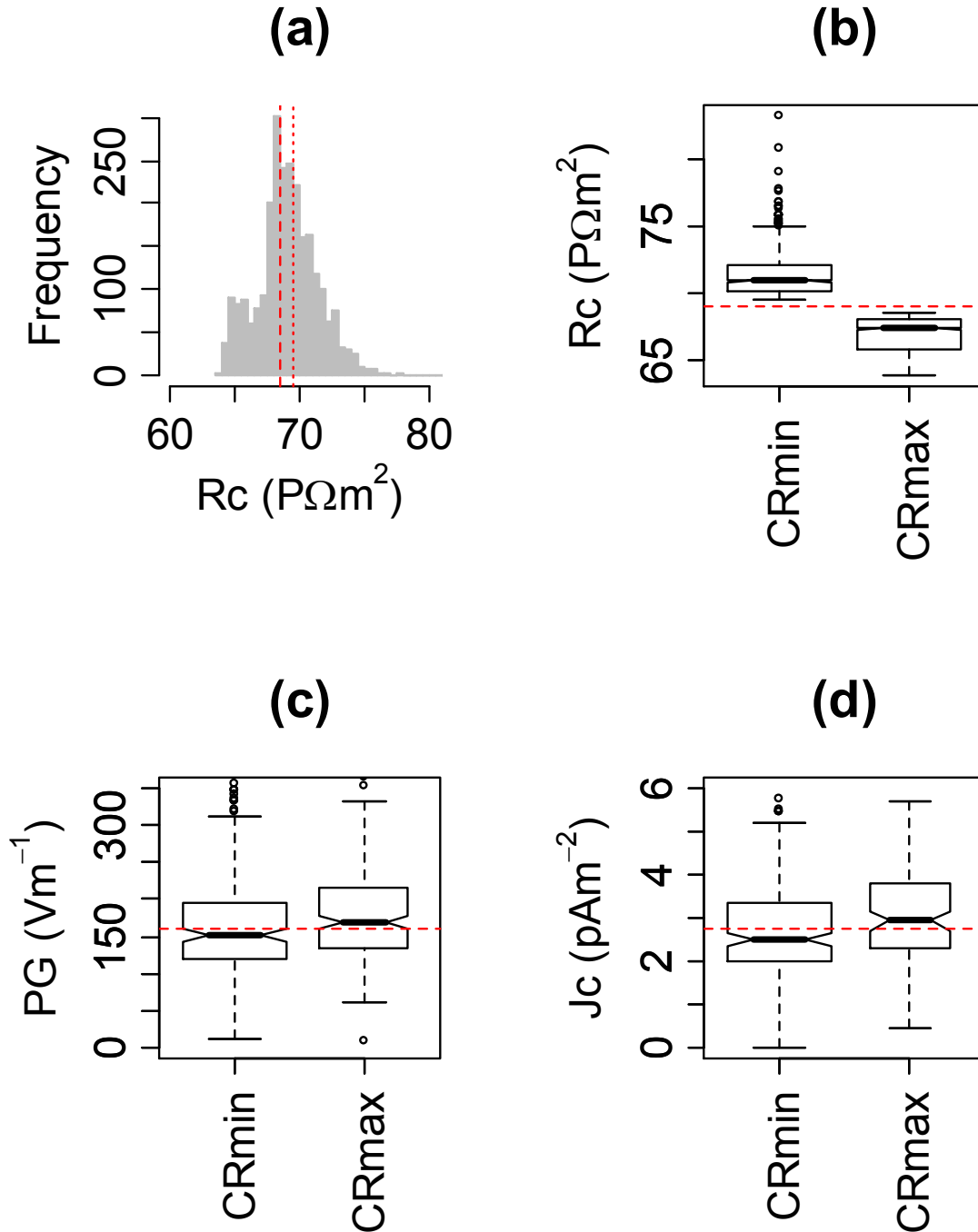


Figure 3. (a) Histogram of calculated columnar resistances  $R_c$  for Lerwick with the upper and lower 40% quantiles marked to distinguish between “CRmin” (dotted line) and “CRmax” (dashed line) respectively. (b), (c), (d) Comparisons of CRmin and CRmax columnar resistances  $R_c$  (b), with measured and seasonally corrected Potential Gradient (c) and conduction current density (d), from Lerwick. Dashed line shows the medians of the undivided data set. (For the boxplots, the box width is proportional to the square root of the number of values in each interval; the box edges and the line in the centre of each box show the upper and lower quartiles and the median respectively. Notches indicate the 95% confidence limits on the medians and the whiskers extend to 1.5 times the inter-quartile range.)

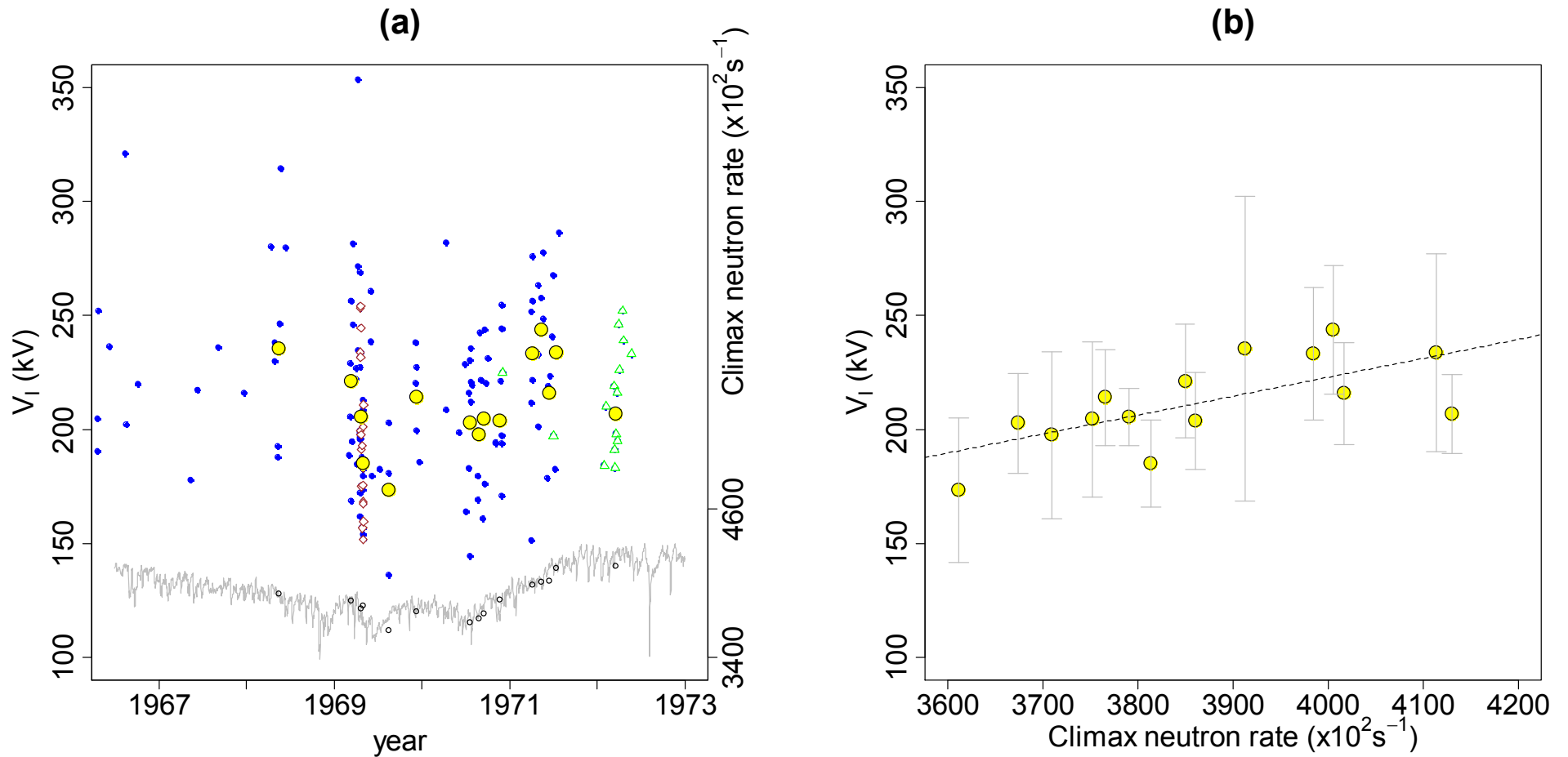


Figure 4. Comparison of ionospheric potential ( $V_1$ ) and neutron counter data at Climax (grey line), measured from 1966-1972. (a)  $V_1$  soundings of Mülheisen from Weissenau, Germany (blue points, individual soundings) and the *Meteor* research ship in the mid-atlantic (brown diamonds, individual soundings), and of Markson from the Bahamas (green triangles, daily averages). Hollow circles show monthly averages for months having 4 or more  $V_1$  points available, with the monthly neutron counter averages using the same days' data as for  $V_1$ . (b) Monthly-averaged  $V_1$  plotted against monthly average neutron count rate. Error bars represent two standard errors. (Individual Mülheisen  $V_1$  soundings have been corrected to equivalent daily values using the Carnegie curve, assuming the sounding to be representative of  $V_1$  at 3.5 hours after launch time.)

**Table 1. Changes in 1978-1985 Lerwick fair weather atmospheric electricity quantities between cosmic ray maximum ( $CR_{max}$ ) and minimum ( $CR_{min}$ )**

<i>location</i>	<i>quantity</i>	<i>median</i>	<i>median value during <math>CR_{min}</math></i> <i>[95% confidence range]</i>	<i>median value during <math>CR_{max}</math></i> <i>[95% confidence range]</i>	<i>change <math>CR_{min}</math> to <math>CR_{max}</math></i>
Climax	neutron count rate (measured)	$3801 \times 10^2 \text{ hr}^{-1}$	$3629 \times 10^2 \text{ hr}^{-1}$ [3622 to 3637] (986 values)	$3932 \times 10^2 \text{ hr}^{-1}$ [3921 to 3943] (982 values)	8.4%
Lerwick	columnar resistance $R_c$ (calculated)	$69 \text{ P}\Omega\text{m}^2$	$70.9 \text{ P}\Omega\text{m}^2$ [70.8 to 71.0] (1019 values)	$67.3 \text{ P}\Omega\text{m}^2$ [67.2 to 67.5] (1012 values)	-5.1%
	potential gradient PG (measured)	$160.5 \text{ Vm}^{-1}$	$151.7 \text{ Vm}^{-1}$ [144.2 to 159.2] (266 values)	$170.0 \text{ Vm}^{-1}$ [160.9 to 179.0] (193 values)	12.0%
	current density $J_c$ (measured)	$2.76 \text{ pA m}^{-2}$	$2.51 \text{ pA m}^{-2}$ [2.36 to 2.67] (202 values)	$2.93 \text{ pA m}^{-2}$ [2.70 to 3.50] (120 values)	16.5%

**Table A1. Effect of sampling time on linear fit in figure 4(b)**

sampling time $h_s$ from launch (hours)	p-value	confidence level
$h_s < -1$	>0.05	
$0 \leq h_s \leq 2$	<0.05	>95%
$2 < h_s < 3$	<0.02	>98%
$3 < h_s < 5$	<0.001	>99.8%
$5 < h_s < 8$	<0.02	>98%
$h_s > 10$	>0.05	